A BLUE-Based Approach to Frequency Recovery in OFDM Receivers with I/Q Imbalance

Antonio A. D'Amico, Michele Morelli, and Marco Moretti
Dipartimento Ingegneria dell'Informazione
University of Pisa
Email: {antonio.damico, michele.morelli, marco.moretti}@unipi.it

***Abstract*—Direct conversion receivers (DCRs) are an effective means to obtain user terminals with reduced cost, size, and power consumption. Their major drawback is the possible insertion of I/Q imbalances in the demodulated signal, which can seriously degrade the performance of conventional synchronization algorithms. In this paper, we investigate the problem of carrier frequency offset (CFO) recovery in an OFDM receiver equipped with a DCR front-end. Our approach is based on the best linear unbiased estimation (BLUE) theory and aims at jointly estimating the CFO, the useful signal component, and its mirror image. In doing so, we exploit knowledge of the pilot symbols transmitted within a conventional repeated training preamble appended in front of each data packet. Two solutions are proposed, and both of them provides the CFO in closed-form, thereby avoiding any grid-search procedure. The accuracy of the proposed methods is assessed in a scenario compliant with the 802.11a WLAN standard. Compared with existing solutions, the novel schemes achieve improved performance at the price of a marginal increase of the processing load.**

I. Introduction

Orthogonal frequency-division multiplexing (OFDM) is a popular multicarrier technology which offers remarkable resilience against multipath distortions, increased spectral efficiency, and the possibility of performing adaptive modulation and coding. Due to such potential advantages, it has been adopted in several wideband commercial systems, including the IEEE 802.11a wireless local area network (WLAN) [1], the IEEE 802.16 wireless metropolitan area network (WMAN) [2] and the 3GPP long-term evolution (LTE) [3]. The use of a direct-conversion receiver (DCR) in combination with the OFDM technology can provide an effective means for the implementation of user terminals with reduced size and power consumption [4]. The price is a higher degree of radio-frequency (RF) imperfections arising from the use of analog in-phase/quadrature (I/Q) low-pass filters (LPF) with mismatched frequency responses, and from local oscillator (LO) signals with amplitude and phase imbalances [5]. If not properly compensated, the I/Q imbalance introduces image interference from mirrored subcarriers, with ensuing limitations of the system performance. In addition to I/Q imperfections, an OFDM receiver is also vulnerable to the carrier frequency offset (CFO) between the incoming waveform and the LO signals, which generates interchannel interference in the demodulated signal.

In recent years, an intense research activity has been conducted to investigate the problem of CFO recovery in OFDM systems plagued by frequency-selective I/Q imperfections. Many available solutions operate in the time-domain and exploit a suitably designed training preamble (TP) appended in front of the data packet [6]–[15]. The main drawback of these methods is that they rely on specific TPs that cannot be found in any OFDM communication standard. In addition, most of them are not computationally efficient as they require a grid-search over the uncertainty frequency interval. Alternative schemes employing the IEEE 802.11a conventional repeated TP can be found in [16]–[20]. In [19] and [20], the useful signal component and its mirror image are interpreted as two independent sinusoidal signals, which are separated by resorting to either the ESPRIT (estimation of signal parameters via rotational invariance technique [21]) or the SAGE (space-alternating generalized expectation-maximization [22]) algorithms, respectively. In [23] the authors show that, at low and medium signal-to-noise ratio (SNR) values, the classical maximum likelihood (CML) frequency estimator derived in [24] for a perfectly balanced receiver performs satisfactorily even in the presence of some I/Q imbalance. Furthermore, in many situations CML exhibits improved accuracy with respect to the joint maximum likelihood (JML) estimator of the CFO, the channel distorted TP and its mirror image, which was originally presented in [11]. The reason is that JML, when applied to a repetitive TP, is subject to a sign ambiguity problem and provides poor results in the presence of small CFO values. A novel frequency estimator is also derived in [23] by exploiting some side-information about the signal-to-image ratio. Finally, a low-complexity scheme for the joint estimation of the CFO, channel impulse response (CIR) and I/Q imbalance is presented in [25] using the long training sequence embedded in the 802.11a preamble.

In this work, we consider an OFDM direct-conversion receiver affected by frequency-selective I/Q imbalances and further investigate the CFO recovery task using a repeated TP. We derive two schemes based on the best linear unbiased estimation (BLUE) principle, which provide the CFO estimate in closed-form without resorting to expensive grid-search procedures. Numerical simulations indicate that the proposed schemes perform satisfactorily even in the presence of severe I/Q imbalances and outperform considerably other existing methods.

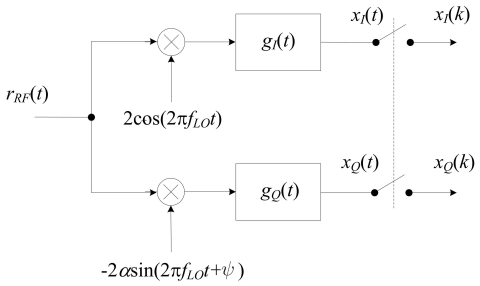

Fig. 1. Basic DCR architecture

II. System model in the presence of CFO and I/Q imbalance

A. DCR architecture

Fig. 1 illustrates the basic structure of a DCR front-end. Here, the received RF waveform $r_{RF}(t)$ is down-converted to baseband using LO signals characterized by an amplitude mismatch α and a phase error ψ. The demodulated signals are then fed to I/Q low-pass filters with different impulse responses $g_I(t)$ and $g_Q(t)$. While LO imperfections give rise to frequency-independent I/Q imbalances, filter mismatches vary over the signal bandwidth, thereby resulting into a frequency-selective imbalance [11]. We call $r(t)$ the complex envelope of $r_{RF}(t)$ with respect to the carrier frequency f_0, and let $\Delta f = f_0 - f_{LO}$ be the offset between the carrier and LO frequencies. Hence, we can write the received waveform as $r_{RF}(t) = \Re\mathrm{e}\{r(t)e^{j2\pi(f_{LO}+\Delta f)t}\}$, with

$$r(t) = s(t) \otimes v(t) + n(t). \tag{1}$$

In the above equation, $s(t)$ and $v(t)$ are the baseband representations of the transmitted signal and propagation channel, respectively, while $n(t)$ is circularly symmetric AWGN with two-sided power spectral density $2N_0$. As shown in Fig. 1, we denote by $x(t) = x_I(t) + jx_Q(t)$ the complex down-converted signal at the output of the mismatched I/Q filters. Then, after standard manipulations we get

$$x(t) = e^{j2\pi\Delta ft}[s(t) \otimes \tilde{h}(t)] + e^{-j2\pi\Delta ft}[s^*(t) \otimes \tilde{q}(t)] + w(t) \tag{2}$$

where the first term is the direct signal component, the second term represents self-image interference, and $w(t)$ accounts for the noise contribution. The equivalent CIRs $\tilde{h}(t)$ and $\tilde{q}(t)$ appearing in (2) can be expressed as [11]

$$\begin{aligned} \tilde{h}(t) &= v(t) \otimes p_+(t)e^{-j2\pi\Delta ft} \\ \tilde{q}(t) &= v^*(t) \otimes p_-(t)e^{j2\pi\Delta ft} \end{aligned} \tag{3}$$

with

$$\begin{aligned} p_+(t) &= \tfrac{1}{2}[g_I(t) + \alpha g_Q(t)e^{-j\psi}] \\ p_-(t) &= \tfrac{1}{2}[g_I(t) - \alpha g_Q(t)e^{j\psi}] \end{aligned} \tag{4}$$

while the noise term $w(t) = w_I(t) + jw_Q(t)$ takes the form

$$w(t) = n(t)e^{j2\pi\Delta ft} \otimes p_+(t) + n^*(t)e^{-j2\pi\Delta ft} \otimes p_-(t). \tag{5}$$

Substituting (4) into (5), it is found that $w_I(t)$ and $w_Q(t)$ are zero-mean Gaussian processes with auto- and cross-correlation functions

$$\begin{aligned} \mathrm{E}\{w_I(t)w_I(t+\tau)\} &= N_0[g_I(\tau) \otimes g_I(-\tau)] \\ \mathrm{E}\{w_Q(t)w_Q(t+\tau)\} &= \alpha^2 N_0[g_Q(\tau) \otimes g_Q(-\tau)] \\ \mathrm{E}\{w_I(t)w_Q(t+\tau)\} &= -\alpha N_0 \sin\psi[g_I(\tau) \otimes g_Q(-\tau)]. \end{aligned} \tag{6}$$

Since the real and imaginary components of $w(t)$ are generally cross-correlated with different auto-correlation functions, we conclude that, in general, the noise process at the ouptut of a DCR front-end is not circularly symmetric.

B. Mathematical model of the received TP

We consider an OFDM burst-mode communication system, where each burst is preceded by a TP to assist the synchronization and channel estimation functions. In contrast to many related works, where the TP is suitably designed to cope with I/Q imbalances [6]- [15], in this study we assume a conventional periodic preamble composed by $M_T \geq 2$ repeated segments. Each segment contains P time-domain samples, which are obtained as the inverse discrete Fourier transform (IDFT) of P pilot symbols $\{c(n); n = 0, 1, \ldots, P-1\}$. Such a preamble is general enough to include both the short training sequence ($M_T = 10$, $P = 16$) and the long training sequence ($M_T = 2$, $P = 64$) of the 802.11a WLAN standard [1]. In the former case, a number $M_G \geq 1$ of segments serve as a cyclic prefix (CP) to avoid interblock interference, while the remaining $M = M_T - M_G$ segments are exploited for synchronization purposes. In the latter case we have $M_G = 0$ since the long training sequence is preceded by its own CP.

At the transmit side, the time-domain samples are fed to a pulse shaping filter with impulse response $h_{TX}(t)$ and signaling interval T_s. The transmitted TP is thus given by

$$s(t) = \frac{1}{\sqrt{P}} \sum_{k=-N_G}^{MP-1} \sum_{n=0}^{P-1} c(n)e^{j2\pi nk/P} h_{TX}(t - kT_s) \qquad 0 \leq t \leq MPT_s \tag{7}$$

where N_G is the CP duration normalized by the signaling period. After propagating through the multipath channel, the received waveform $x(t)$ plagued by CFO and frequency-selective I/Q imbalances is sampled with period T_s, thereby producing the MP samples

$$x[l] = e^{jl\phi}[s(t) \otimes \tilde{h}(t)]_{t=lT_s} + e^{-jl\phi}[s^*(t) \otimes \tilde{q}(t)]_{t=lT_s} + w[l] \tag{8}$$

where we have defined

$$\phi = 2\pi\Delta fT_s. \tag{9}$$

We denote by $h(t) = h_{TX}(t) \otimes \tilde{h}(t)$ and $q(t) = h_{TX}(t) \otimes \tilde{q}(t)$ the overall CIRs for the useful signal component and its mirror image, respectively. Then, assuming that $h(t)$ and $q(t)$ have support $[0, LT_s)$, with $L \leq N_G$, from (7) and (8) we get

$$\begin{aligned} x[l] = &\frac{e^{jl\phi}}{\sqrt{P}} \sum_{k=0}^{L-1} h[k] \sum_{n=0}^{P-1} c(n)e^{j2\pi n(l-k)/P} \\ &+ \frac{e^{-jl\phi}}{\sqrt{P}} \sum_{k=0}^{L-1} q[k] \sum_{n=0}^{P-1} c^*(n)e^{-j2\pi n(l-k)/P} + w[l] \end{aligned} \tag{10}$$

with $h[k] = h(kT_s)$ and $q[k] = q(kT_s)$. To proceed further, we arrange the received samples $x[l]$ into M vectors $\{\mathbf{x}_m; m = 0, 1, \ldots, M-1\}$, where $\mathbf{x}_m = (x[mP], x[mP+1], \ldots, x[mP+P-1])^T$ collects the P samples belonging to the mth received TP segment. Taking (10) into account yields

$$\begin{aligned}\mathbf{x}_m &= e^{jmP\phi}\mathbf{\Gamma}_P(\phi)\mathbf{F}_P\mathbf{C}\mathbf{G}_2\mathbf{h} \\ &\quad + e^{-jmP\phi}\mathbf{\Gamma}_P(-\phi)\mathbf{F}_P^*\mathbf{C}^*\mathbf{G}_2^*\mathbf{q} + \mathbf{w}_m\end{aligned} \tag{11}$$

where $\mathbf{h} = (h[0], h[1], \ldots, h[L-1])^T$ and $\mathbf{q} = (q[0], q[1], \ldots, q[L-1])^T$ are the $L-$dimensional CIR vectors, $\mathbf{w}_m = (w[mP], w[mP+1], \ldots, w[mP+P-1])^T$ represents the noise contribution, $\mathbf{\Gamma}_P(\phi) = \mathrm{diag}\{e^{jl\phi}, l = 0, 1, \ldots, P-1\}$, $\mathbf{C} = \mathrm{diag}\{c(n), n = 0, 1, \ldots, P-1\}$, $\mathbf{G}_2$ is a $(P \times L)-$dimensional matrix with entries

$$[\mathbf{G}_2]_{n,k} = e^{-j2\pi(n-1)(k-1)/P} \tag{12}$$

and, finally, $\mathbf{F}_P$ is the unitary $P-$point IDFT matrix with entries

$$[\mathbf{F}_P]_{n,k} = \frac{1}{\sqrt{P}} e^{j2\pi(n-1)(k-1)/P} \quad n, k = 1, 2, \ldots, P. \tag{13}$$

III. BLUE-BASED CFO RECOVERY

In this Section, we propose an estimation algorithm which is able to provide the CFO in closed-form. Our scheme is derived following a best linear unbiased estimation (BLUE) approach, and assumes that $\mathbf{w}_m$ is a zero-mean circularly symmetric Gaussian (ZMCSG) complex vector with covariance matrix $\sigma_w^2\mathbf{I}_P$. Although this assumption holds true only in a perfectly balanced DCR architecture, it has been used even in the presence of non-negligible I/Q imbalances to derive novel frequency recovery schemes [26]. We point out that in our study the white noise assumption is adopted only to derive the CFO estimators, while the true noise statistics shown in (6) are employed in the numerical analysis to assess the system performance in a more realistic scenario.

To proceed further, we make the following approximation

$$\mathbf{\Gamma}_P(\phi) \simeq e^{j(P-1)\phi/2}\mathbf{I}_P \tag{14}$$

which amounts to replacing the linearly increasing phase shift $l\phi$ for $l = 0, 1, \ldots, P-1$ by its average value $(P-1)\phi/2$. This yields

$$\begin{aligned}\mathbf{x}_m &\simeq e^{j(2mP+P-1)\phi/2}\mathbf{F}_P\mathbf{C}\mathbf{G}_2\mathbf{h} \\ &\quad + e^{-j(2mP+P-1)\phi/2}\mathbf{F}_P^*\mathbf{C}^*\mathbf{G}_2^*\mathbf{q} + \mathbf{w}_m\end{aligned} \tag{15}$$

which can also be written in a more compact form as

$$\mathbf{x}_m = \mathbf{T}\mathbf{u}_m + \mathbf{w}_m \tag{16}$$

where $\mathbf{u}_m$ is a $2L-$dimensional vector expressed by

$$\mathbf{u}_m = \begin{bmatrix} e^{j(2mP+P-1)\phi/2}\mathbf{h} \\ e^{-j(2mP+P-1)\phi/2}\mathbf{q} \end{bmatrix} \tag{17}$$

and $\mathbf{T}$ is the following matrix of dimension $P \times (2L)$

$$\mathbf{T} = [\mathbf{T}_1 \quad \mathbf{T}_1^*] \tag{18}$$

with $\mathbf{T}_1 = \mathbf{F}_P\mathbf{C}\mathbf{G}_2$. From the simplified model (16), the ML estimate of $\mathbf{u}_m$ is computed as

$$\hat{\mathbf{u}}_m = (\mathbf{T}^H\mathbf{T})^{-1}\mathbf{T}^H\mathbf{x}_m. \tag{19}$$

Then, recalling the structure of $\mathbf{u}_m$ shown in (17), we observe that the first L elements of $\hat{\mathbf{u}}_m$ provide an estimate of $e^{j(2mP+P-1)\phi/2}\mathbf{h}$, while the last L elements provide an estimate of $e^{-j(2mP+P-1)\phi/2}\mathbf{q}$. Since in a practical scenario the energy of $\mathbf{q}$ is typically much smaller than the energy of $\mathbf{h}$, in the sequel we only exploit the first part of $\hat{\mathbf{u}}_m$ $(m = 0, 1, \ldots, M-1)$ to retrieve the CFO. This approach has the remarkable advantage of reducing the system complexity without leading to any significant loss in estimation accuracy. Hence, substituting (16) into (19) and denoting by $\boldsymbol{\xi}_m$ the first L entries of $\hat{\mathbf{u}}_m$ yields

$$\boldsymbol{\xi}_m = e^{j(2mP+P-1)\phi/2}\mathbf{h} + \boldsymbol{\eta}_m \tag{20}$$

where $\boldsymbol{\eta}_m$ is a zero-mean Gaussian vector with 'covariance matrix $\mathbf{C}_\eta = \sigma_w^2\mathbf{K}$ and $\mathbf{K}$ is an $L-$dimensional matrix with entries $[\mathbf{K}]_{i,j} = [(\mathbf{T}^H\mathbf{T})^{-1}]_{i,j}$ for $1 \le i, j \le L$.

Letting $\mathbf{y}_m = \mathbf{K}^{-1/2}\boldsymbol{\xi}_m$ and $\mathbf{h}_{eq} = \mathbf{K}^{-1/2}\mathbf{h}$, we get

$$\mathbf{y}_m = e^{j(2mP+P-1)\phi/2}\mathbf{h}_{eq} + \mathbf{n}_m \tag{21}$$

where $\mathbf{n}_m = \mathbf{K}^{-1/2}\boldsymbol{\eta}_m$ is a zero-mean Gaussian vector with covariance matrix $\mathbf{C}_n = \sigma_w^2\mathbf{I}_L$. Now, consider the correlations $\{R(m); 1 \le m \le M-1\}$ defined as

$$R(m) = \sum_{k=m}^{M-1} \mathbf{y}_{k-m}^H\mathbf{y}_k \qquad 1 \le m \le M-1. \tag{22}$$

Substituting (21) into (22) produces

$$R(m) = (M-m)\left\|\mathbf{h}_{eq}\right\|^2 e^{jmP\phi}[1+\gamma(m)] \quad 1 \le m \le M-1 \tag{23}$$

with

$$\gamma(m) = \frac{1}{(M-m)\left\|\mathbf{h}_{eq}\right\|^2}\sum_{k=m}^{M-1}[\mathbf{h}_{eq}^H\mathbf{n}_k + \mathbf{n}_{k-m}^H\mathbf{h}_{eq} + \mathbf{n}_{k-m}^H\mathbf{n}_k]. \tag{24}$$

Inspection of (23) reveals that the unknown parameter ϕ is linearly related to the argument of $R(m)$. Hence, we define the angles

$$\theta(m) = \arg\{R(m)R^*(m-1)\} \qquad 1 \le m \le M-1 \tag{25}$$

where $R(0)$ is set to unity. Furthermore, we assume large SNR values such that $|\gamma(m)| \ll 1$ and $\arg\{1+\gamma(m)\} \simeq \gamma_I(m)$, with $\gamma_I(m)$ being the imaginary part of $\gamma(m)$. In these circumstances, from (23) we have

$$\theta(m) \simeq [P\phi + \gamma_I(m) - \gamma_I(m-1)]_{2\pi} \tag{26}$$

where $[x]_{2\pi}$ denotes the value of x reduced to the interval $[-\pi, \pi)$. If ϕ is adequately smaller than π/P, the quantity in square brackets in (26) is (with high probability) less than π and $\theta(m)$ reduces to

$$\theta(m) = P\phi + \eta(m) \tag{27}$$

with $\eta(m) = \gamma_I(m) - \gamma_I(m-1)$. Based on model (27), the BLUE of ϕ as a function of the observation variables $\boldsymbol{\theta} = [\theta(1), \theta(2), \ldots, \theta(M-1)]^T$ is given by [27]

$$\hat{\phi}_{BLUE} = \frac{1}{P} \sum_{m=1}^{M-1} \alpha(m)\theta(m) \tag{28}$$

where $\alpha(m)$ is the mth element of

$$\boldsymbol{\alpha} = \frac{1}{\mathbf{1}^T \mathbf{C}_\eta^{-1} \mathbf{1}} \mathbf{C}_\eta^{-1} \mathbf{1} \tag{29}$$

and $\mathbf{C}_\eta$ is the covariance matrix of $\boldsymbol{\eta} = [\eta(1), \eta(2), \ldots, \eta(M-1)]^T$. Denoting by $\mathbf{C}_{\gamma_I}$ the covariance matrix of $\boldsymbol{\gamma}_I = [\gamma_I(1), \gamma_I(2), \ldots, \gamma_I(M-1)]^T$ and taking into account that $\gamma_I(0) = 0$, we have (see equation (30) at top of next page)

After lengthy calculations (not reported here for space limitations), we find that

$$\mathbf{C}_{\gamma_I} = \frac{\sigma_w^2}{\|\mathbf{h}_{eq}\|^2} (\mathbf{B}_{SN} + \mathbf{B}_{NN}) \tag{31}$$

where $\mathbf{B}_{SN}$ is an $(M-1) \times (M-1)$ matrix with entries

$$[\mathbf{B}_{SN}]_{m,\ell} = \frac{M - \max(m,\ell) - (M-m-\ell)\mathrm{u}(M-m-\ell)}{(M-m)(M-\ell)} \tag{32}$$

$\mathrm{u}(n)$ being the unit step function, whereas

$$[\mathbf{B}_{NN}]_{m,\ell} = \frac{\sigma_w^2}{2\|\mathbf{h}_{eq}\|^2 (M-m)} \delta(m-\ell) \tag{33}$$

Taking (30) and (31) into account yields

$$\boldsymbol{\alpha} = \frac{1}{\mathbf{1}^T \check{\mathbf{C}}_\eta^{-1} \mathbf{1}} \check{\mathbf{C}}_\eta^{-1} \mathbf{1} \tag{34}$$

where $\check{\mathbf{C}}_\eta = \mathbf{C}_\eta / (\sigma_w^2 / \|\mathbf{h}_{eq}\|^2)$ is computed through (30) by replacing, in the right-hand side, $\mathbf{C}_{\gamma_I}$ with $\mathbf{B} = \mathbf{B}_{SN} + \mathbf{B}_{NN}$.

The major drawback of algorithm (28) is that the computation of $\boldsymbol{\alpha}$ requires knowledge of the ratio $\sigma_w^2 / \|\mathbf{h}_{eq}\|^2$, as results from (33). An alternative approach consists in neglecting $\mathbf{B}_{NN}$ in (31), which amounts to approximating (24) with

$$\gamma(m) \approx \frac{1}{(M-m)\|\mathbf{h}_{eq}\|^2} \sum_{k=m}^{M-1} [\mathbf{h}_{eq}^H \mathbf{n}_k + \mathbf{n}_{k-m}^H \mathbf{h}_{eq}]. \tag{35}$$

In such a case, since $(M-m)\gamma_I(m) = m\gamma_I(M-m)$ for $m = 1, \ldots, M/2-1$, it can be shown that the last $M/2-1$ elements of $\boldsymbol{\theta}$ can be obtained through a linear transformation of the first $M/2-1$. This means that, in deriving the BLUE on the basis of (35), we only need to consider $\theta(m)$ for $m = 1, 2, \ldots, M/2$. Accordingly, we have

$$\hat{\phi}_{BLUE-S} = \frac{1}{P} \sum_{m=1}^{M/2} \beta(m)\theta(m) \tag{36}$$

where the weights $\beta(m)$ can be computed in closed-form, as shown in [28], and are given by

$$\beta(m) = 3\frac{4(M-m)(M-m+1) - M^2}{2M(M^2-1)} \tag{37}$$

Clearly, they depend neither on σ_w^2 nor on $\mathbf{h}_{eq}$.

IV. Simulation results

Computer simulations have been run to assess the performance of the proposed methods in an OFDM WLAN system compliant with the IEEE 802.11a standard [1]. The DFT size is $N = 64$, while the sampling interval is set to $T_s = 50$ ns. This corresponds to a transmission bandwidth of 20 MHz with a subcarrier distance of 312.5 kHz. The synchronization schemes are applied to the short training sequence placed in front of each frame. This sequence carries $N_p = 12$ non-zero pilot symbols and is divided into $M_T = 10$ repeated parts, each containing $P = 16$ samples. After discarding the first two segments as the CP of the TP, the remaining $M = 8$ segments are exploited for CFO recovery. The propagation channel has discrete-time impulse response $\mathbf{v} = [v(0), v(1), \ldots, v(L_v-1)]^T$ of order L_v. The entries of $\mathbf{v}$ follow a circularly-symmetric Gaussian distribution with an exponentially decaying power delay profile

$$\mathrm{E}\{|v(k)|^2\} = \sigma_v^2 \exp(-k/L_v) \qquad k = 0, 1, \ldots, L_v - 1 \tag{38}$$

where $L_\nu = 4$ and σ_v^2 is chosen such that $\mathrm{E}\{\|\mathbf{v}\|^2\} = 1$. Both frequency independent and frequency selective RF imperfections are considered. Unless otherwise specified, the LO-induced imbalance is characterized by $\alpha = 1$ dB and $\psi = 5$ degrees, while the receive I/Q filters have discrete-time impulse responses $\mathbf{g}_I = [0, 1, \mu]^T$ and $\mathbf{g}_Q = [\mu, 1, 0]^T$ with $\mu = 0.1$. These values have been previously adopted in the related literature [11] and represent a plausible model for I/Q mismtaches. The TX filter has ideal response $h_{TX}(nT_s) = \delta[n]$, which results into overall CIRs $h[k]$ and $q[k]$ having support $k = 0, 1, \ldots, L-1$, with $L = L_v + 2$. In addition to the aforementioned simulation set-up, in our study we also consider a more general scenario wherein a coefficient $\rho \in [0, 4]$ is used to specify the values of the I/Q imbalance parameters as $\mu = 0.1\rho$, $\alpha = 1 + 0.122\rho$ and $\psi = 5\rho$ degrees. This allows one to assess the sensitivity of the considered schemes to the amount of RF imperfections, with $\rho = 0$ corresponding to an ideal situation where no I/Q imbalance is present.

Assuming a carrier frequency of 5 GHz and an oscillator instability of ± 30 parts-per-million (ppm), the maximum value of ϕ is found to be $\phi^{(\max)} = 0.015\pi$. This value falls well within the estimation range of BLUE, which is given by $|\phi| \leq \pi/P = 0.0625\pi$.

The accuracy of the proposed synchronization schemes (28) and (36) is assessed in terms of their mean square estimation error (MSEE). The estimated parameter is the CFO normalized by the subcarrier spacing, which is defined as $\nu = NT_s\Delta f$ or, equivalently, $\nu = N\phi/(2\pi)$. Recalling that $\phi^{(\max)} = 0.015\pi$, the uncertainty range of ν is given by $|\nu| \leq 0.48$. Comparisons are made with alternative ML-oriented methods, including the CML [24] and JML [11].

Fig. 2 illustrates the MSEE of the CFO estimators as a function of ν measured at SNR=15 dB. We see that JML performs poorly for small CFO values, while the accuracy of the other schemes depends weakly on ν. The reason for

$$[\mathbf{C}_\eta]_{m,\ell} = \begin{cases} [\mathbf{C}_{\gamma_I}]_{m,\ell} - [\mathbf{C}_{\gamma_I}]_{m,\ell-1} - [\mathbf{C}_{\gamma_I}]_{m-1,\ell} + [\mathbf{C}_{\gamma_I}]_{m-1,\ell-1} & m,\ell = 2,\ldots,M-1, \\ [\mathbf{C}_{\gamma_I}]_{m,\ell} - [\mathbf{C}_{\gamma_I}]_{m,\ell-1} & m = 1 \quad \ell = 2,\ldots,M-1, \\ [\mathbf{C}_{\gamma_I}]_{m,\ell} - [\mathbf{C}_{\gamma_I}]_{m-1,\ell} & m = 2,\ldots,M-1 \quad \ell = 1, \\ [\mathbf{C}_{\gamma_I}]_{m,\ell} & m = \ell = 1. \end{cases} \tag{30}$$

the poor performance of JML when ν approaches zero is that this scheme aims at jointly estimating the channel distorted signal component $\mathbf{a} = \mathbf{\Gamma}_P(\phi)\mathbf{F}_P\mathbf{C}\mathbf{G}_2\mathbf{h}$ and its mirror image $\mathbf{b} = \mathbf{\Gamma}_P(-\phi)\mathbf{F}_P^*\mathbf{C}^*\mathbf{G}_2^*\mathbf{q}$ without effectively exploiting their mathematical model. Since in the absence of any CFO the mth received TP segment in (11) becomes $\mathbf{x}_m = \mathbf{a}+\mathbf{b}+\mathbf{w}_m$, there is no possibility for JML to get individual estimates of $\mathbf{a}$ and $\mathbf{b}$ in this specific situation. In contrast, the proposed algorithms BLUE and BLUE-S (which have virtually the same performance) can work satisfactorily for any CFO value as they exploit the inherent structure of $\mathbf{a}$ and $\mathbf{b}$, which makes these vectors resolvable even when $\nu = 0$. It is worth observing that CML, which is derived by ignoring the presence of I/Q imbalances, performs remarkably better than JML for $\nu < 0.15$. The results of Fig. 3 are obtained under the same operating conditions of Fig. 2, except that the SNR is now set to 30 dB. In such a case, the performance of CML exhibits large fluctuations as a function of ν, while the proposed schemes provide a very good accuracy irrespective of the CFO value. Again, JML performs poorly when ν approaches zero due to the impossibility of resolving vectors $\mathbf{a}$ and $\mathbf{b}$. Figs. 4 and 5 show the MSEE of the CFO estimators as a function of ρ with ν uniformly distributed over the interval $[-0.5, 0.5]$. The SNR is 15 dB in Fig. 4 and 30 dB in Fig. 5. These results indicate that the accuracy of CML is significantly affected by the amount of I/Q imbalances. As for the proposed schemes, they exhibit a remarkable resilience against RF imperfections at an SNR of 15 dB, while some performance degradation is observed for SNR=30 dB at high values of ρ. Nonetheless, the BLUE-based algorithms largely outperform both JML and CML. Fig. 6 illustrates the accuracy of the investigated schemes as a function of the SNR when $\rho = 1$ and ν varies uniformly within the interval $[-0.5, 0.5]$. Comparisons are also made with the reduced-complexity estimator (RCE) proposed

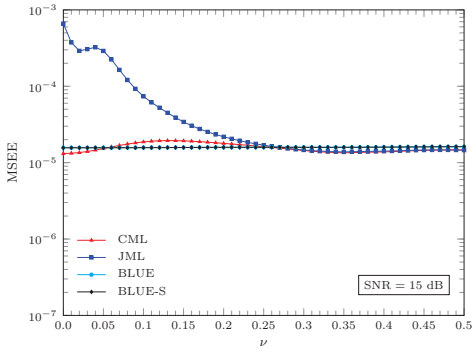

Fig. 2. Accuracy of the CFO estimators vs. ν with SNR=15 dB

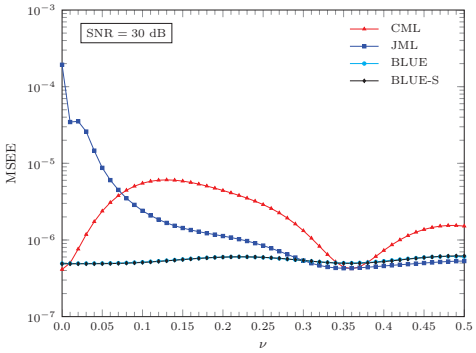

Fig. 3. Accuracy of the CFO estimators vs. ν with SNR=30 dB

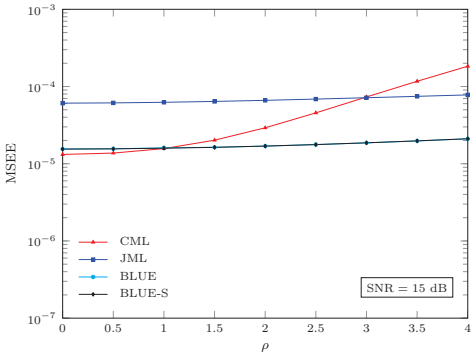

Fig. 4. Accuracy of the CFO estimators vs. ρ with SNR=15 dB

in [25]. Although RCE was originally designed to operate with a TP composed of two identical halves, it can be applied to the 802.11a short training sequence as well by considering such a sequence as the concatenation of two repeated segments $[\mathbf{x}_0^T \ \mathbf{x}_1^T \cdots \mathbf{x}_{M/2-1}^T]^T$ and $[\mathbf{x}_{M/2}^T \ \mathbf{x}_{M/2+1}^T \cdots \mathbf{x}_{M-1}^T]^T$. As is seen, the proposed schemes achieve a substantial gain with respect to JML and RCE. As for the CML algorithm, it has good performance when SNR$<$15 dB, while it is plagued by a considerable floor at larger SNR values.

V. Conclusions

We analyzed the CFO estimation problem in an OFDM receiver with frequency-selective I/Q imbalances. In doing so, we assumed that a repeated training preamble is available in front of each data packet to assist the synchronization task. By exploiting knowledge of the pilot symbols embedded in the preamble, we derived two estimators based on the best linear unbiased estimation theory. Both of them provide the CFO estimate in closed-form, dispensing from any grid-search procedure. Compared to existing alternatives (CML, RCE, JML), the proposed schemes exhibit a remarkable improvement of

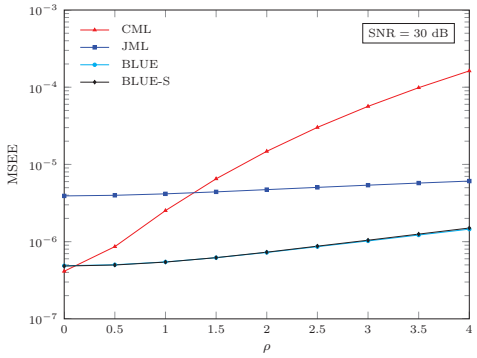

Fig. 5. Accuracy of the CFO estimators vs. ρ with SNR=30 dB

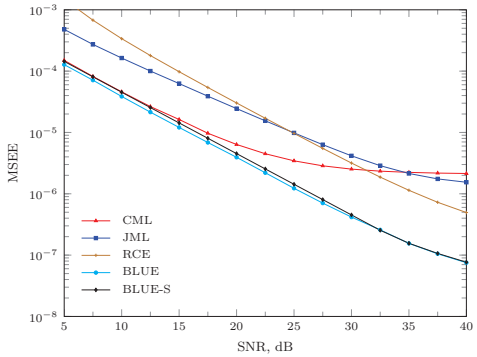

Fig. 6. Accuracy of the CFO estimators vs. SNR

the system performance at the price of a tolerable increase of the computational load.

REFERENCES

[1] *Wireless LAN medium access control (MAC) and physical layer (PHY) specifications, higher speed physical layer extension in the 5 GHz band, IEEE 802.11 WG*, Sep. 1999, Supplement to IEEE 802.11 Standard.

[2] *IEEE standard for local and metropolitan area networks, Part16: Air Interface for Fixed and Mobile Broadband Wireless Access Systems*, IEEE Std. 802.16, 2004.

[3] *Evolved universal terrestrial radio access (E-UTRA); physical channels and modulation*, 3GPP TS 36.211, 2012.

[4] W. Namgoong and T. H. Meng, "Direct-conversion RF receiver design", *IEEE Trans. on Commun.*, vol. 49, n. 3, pp. 518-529, Mar. 2001.

[5] M. Valkama, M. Renfors, and V. Koivunen, "Advanced methods for I/Q imbalance compensation in communication receivers", *IEEE Trans. on Signal Processing*, vol. 49, pp. 2335-2344, Oct. 2001.

[6] F. Yan, W.-P. Zhu, and M. O. Ahmad, "Carrier Frequency Offset Estimation for OFDM Systems with I/Q Imbalance", in Proc. of *47th IEEE Midwest Symposium on Circuits and Systems*, *MWSCAS '04*, vol. 2, pp. 633-636, July 2004.

[7] L. Lanante Jr., M. M. Kurosaki, and H. Ochi, "Low complexity compensation of frequency dependent I/Q imbalance and carrier frequency offset for direct conversion receiver", in *Proc. of IEEE Inter. Symp. on Circuits and Systems (ISCAS) 2010*, pp. 2067-2070, June 2010.

[8] E. L.-Estraviz, S. De Rore, F. Horlin, and L. Van der Perre, "Joint Estimation of Carrier Frequency Offset and IQ Imbalance for 4G Mobile Wireless Systems", in *Proc. of Int. Conf. on Commun. (ICC2006)*, vol. 5, pp. 2066-2071, June 2006.

[9] Y.-C. Pan and S.-M. Phoong, "A new algorithm for carrier frequency offset estimation in the presence of I/Q imbalance", in *Proc. of IEEE Vehic. Techn. Conf. (VTC 2010-Spring)*, pp. 1-5, Apr. 2010.

[10] M. Morelli and M. Moretti, " Carrier frequency offset estimation for OFDM direct-conversion receivers" , *IEEE Trans. on Wireless Commun.*, vol. 11, n. 7, pp. 2670-2679, Jul. 2012.

[11] G. Xing, M. Shen, and H. Liu, "Frequency Offset and I/Q Imbalance Compensation for Direct-Conversion Receivers", *IEEE Trans. on Wireless Commun.*, vol. 4, pp. 673-680, March 2005.

[12] J. Park, Y. Lee, and H. Park, "Preamble Design for Joint Estimation of CFO and I/Q Imbalance for Direct Conversion OFDM System", *IET Communications*, vol. 3, pp. 597-602, 2009.

[13] C.-J. Hsu, R. Cheng, and W.-H- Sheen, "Joint least squares estimation of frequency, DC offset, I-Q imbalance, and channel in MIMO receivers", *IEEE Trans. on Vehic. Techn.*, vol. 58, no. 5, pp. 2201-2213, June 2009.

[14] X. Cai, Y.-C. Wu, H. Lin, and K. Yamashita, "Estimation and compensation of CFO and I/Q imbalance in OFDM systems under timing ambiguity", *IEEE Trans. on Vehic. Techn.*, vol. 60, pp. 1200-1205, Mar. 2011.

[15] H. Lin, X. Zhu, and K. Yamashita, "Low-complexity pilot-aided compensation for carrier frequency offset and I/Q imbalance", *IEEE Trans. on Commun.*, vol. 58, pp. 448-452, Feb. 2010.

[16] Y.-C. Pan and S.-M. Phoong, "A time-domain joint estimation algorithm for CFO and I/Q imbalance in wideband direct-conversion receivers", *IEEE Trans. on Wireless Commun.*, vol. 11, n. 7, pp. 2353-2361, July 2012.

[17] X. Wang, Y. Xue, L. Liu, F. Ye, and J. Ren, "Carrier frequency offset estimation in the presence of I/Q mismatch for wideband OFDM systems", in *Proc. of IEEE 55th Int. Symp. on Circuits and Systems (MWSCAS)*, pp. 924-927, 2012.

[18] R. Kume, H. Lin, and K. Yamashita, "Repeated Preamble Based Carrier Frequency Offset Estimation in the Presence of I/Q Imbalance", in *Proc. of IEEE Int. Conf. on Commun. (ICC 2012)*, pp. 4867-4871, 2012.

[19] M. Morelli, M. Moretti, and H. Lin, "ESPRIT-based carrier frequency offset estimation for OFDM direct-conversion receivers", *IEEE Commun. Letters*, vol. 17, n. 8, pp. 1513-1516, Aug. 2013.

[20] M. Morelli and M. Moretti, "A SAGE approach to frequency recovery in OFDM direct-conversion receivers", *IEEE Commun. Letters*, vol. 18, n. 4, pp. 536-539, Apr. 2014.

[21] U. Tureli, H. Liu, and M. Zoltowski,"OFDM blind carrier offset estimation: ESPRIT", *IEEE Trans. Commun.*, vol. 48, n. 9, pp. 1459-1461, Sept. 2000.

[22] J. A. Fessler and A. O. Hero, "Space-alternating generalized expectation-maximization algorithm", *IEEE Trans. on Signal Processing*, vol. 42, n. 10, pp. 2664-2677, Oct. 1994.

[23] A. A. D'Amico, L. Marchetti, M. Morelli, and M. Moretti, "Frequency estimation in OFDM direct-conversion receivers using a repeated preamble", *IEEE Trans. on Commun.*, vol. 64, n. 3, pp. 1246-1258, Mar. 2016.

[24] M. Ghogho, A. Swami, and P. Ciblat, "Training design for CFO estimation in OFDM over correlated multipath fading channels", in Proc. of *Global Telecommun. Conf. (GLOBECOM) 2007*, pp 2821-2825, 2007.

[25] M. Asim, M. Ghogho, and D. McLernon, "OFDM receiver design in the presence of frequency selective I/Q imbalance and CFO", in *Proc. of 21st European Signal Proc. Conf. (EUSIPCO 2013)*, Marrakech, Sept. 2013.

[26] G.-T. Gil, I.-H. Sohn, J.-K. Park, and Y. H. Lee, "Joint ML estimation of carrier frequency, channel, I/Q mismatch, and DC offset in communication receivers", *IEEE Trans. on Vehic. Techn.*, vol. 54, pp. 338-349, Jan. 2005.

[27] S. M. Kay, *Fundamentals of Statistical Signal Processing: Estimation Theory*, Englewood Cliffs, NJ: Prentice Hall, 1993.

[28] M. Morelli and U. Mengali, "An improved frequency offset estimator for OFDM applications", *IEEE Commun. Lett.*, vol. 3, n. 3, pp. 75-77, Mar. 1999.